Unknotting the interactive effects of learning processes on cultural evolutionary dynamics

Journal:	*Evolutionary Human Sciences*
Manuscript ID	EHS-RES-2019-0019.R1
Manuscript Type:	Research Article
Date Submitted by the Author:	n/a
Complete List of Authors:	Scanlon, Lauren; Durham University, Department of Anthropology Lobb, Andrew; Durham University, Mathematical Sciences Tehrani, Jamie; Durham University, Department of Anthropology Kendal, Jeremy; University of Durham, Anthropology
Keywords:	cultural evolution, social learning, material culture, copying error, knots, approximate Bayesian computation

UNKNOTTING THE INTERACTIVE EFFECTS OF LEARNING PROCESSES ON CULTURAL EVOLUTIONARY DYNAMICS

LAUREN A. SCANLON[1,2], ANDREW LOBB[1], JAMSHID J. TEHRANI[2], JEREMY R. KENDAL[2]
[1]DEPARTMENT OF MATHEMATICS, DURHAM UNIVERSITY
[2]DEPARTMENT OF ANTHROPOLOGY AND DURHAM CULTURAL EVOLUTION RESEARCH CENTRE, DURHAM UNIVERSITY
CORRESPONDENCE EMAIL: JEREMY.KENDAL@DURHAM.AC.UK;
APPROX. WORDCOUNT: 4,700

ABSTRACT. Forms of non-random copying error provide sources of inherited variation yet their effects on cultural evolutionary dynamics are poorly understood. Focusing on variation in granny and reef knot forms, we present a mathematical model that specifies how these variant frequencies are affected by non-linear interactions between copying fidelity, mirroring, handedness and repetition biases. Experiments on adult humans allowed these effects to be estimated using Approximate Bayesian Computation and the model is iterated to explain the prevalence of granny over reef knots in the wild. Our study system also serves to show conditions under which copying fidelity drives heterogeneity in cultural variants at equilibrium, and that interaction between unbiased forms of copying error can skew cultural variation.

1. Introduction

Scholars studying the evolution of human tools have noted that forms of copying error may affect variation in the manufactured forms. For instance, computational and experimental simulation studies show how random copying error that is imperceptible to the learner can result in amplified population-level variation over generations (Eerkens and Lipo, 2005; Kempe et al., 2012). But the relationship between variation in behaviour and the resultant variation in artefacts is not necessarily linear. By mathematical derivation, Hamilton and Buchanan (2009) show that if the magnitude of normally distributed copying error is proportional to the copied object, variation in artefact design evolves through geometric Brownian motion and the mean of the artefact distribution drifts to the left. Thus random copying error can have non-random evolutionary consequences.

While unbiased, normally distributed error can affect evolutionary dynamics, it is plausible that forms of copying error may be non-random and that the accumulation of these errors over generations can affect artefact variation. For example, Kempe et al. (2012) provide putative evidence that artefact size may increase or decrease over generations of reproduction depending on whether the object is constructed by reductive or additive techniques, respectively. Multiple forms of copying error may contribute to artefact construction. For instance, if the learner has to copy a bilaterally symmetrical action, they may attempt the mirror image of the demonstrated action (an instantiation of the correspondence problem; Heyes and Bird 2007) and, in addition, their choice of action could be affected by their own handedness (Laland et al., 1995). If the behaviour includes a sequence of actions, the learner may be inclined to repeat the action they just performed over copying a similar but different action. These forms of copying error may apply across a wide variety of contexts, from motor patterns in tool production, writing, painting and sculpture to athletic activities such as dance or sporting techniques.

Our project concerns the effects of copying errors on the cultural evolution of knot tying. Ashley (1993) collated over 3,800 examples of knots used for a wide variety of functions, ranging from the simple overhand knot which is characterised by only three crossing points, to extremely complex knots with at least 16 crossings. Nonetheless, only a small proportion of all possible knots are actually used and it is unlikely that only these knots could satisfy functional requirements (Scanlon, 2016). Thus the observed variation may have been contingent not only on functional sufficiency but also on modes of social transmission, perceived risk of modifying a knot, the use of knot structures as symbolic markers and learning processes that result in systematic copying errors.

Our study focuses on this latter effect for a family of simple knots which are the composition of overhand knots. These knots can take different forms, characterised by their handedness, which, despite their simplicity, are susceptible to being copied incorrectly. Systematic copying errors across generations of learners may have affected variation not only in these simple knots, but also in more complex knots which include overhand knot structures.

The composition of overhand knots (Alexander-Briggs notation: $3_1\#3_1$) is formed of two trefoil knots (A-B notation: 3_1), each of which is tied by feeding one end of a string through a loop and can take either a right- (R) or left-handed (L) form (Figure 1). The composition of two left- or right-handed trefoils are commonly known as granny knots (LL or RR), while the compositions of a left- and a right-handed trefoil are classed as reef knots (LR or RL). Originating approximately 300kbp and preserved from 5500 bp (Van der Kleij, 1998; Warner and Bednarik, 1998), these knots are a relatively ubiquitous technology (Ashley, 1993). A common use of the composition of overhand knots is to tie shoelaces with an overhand knot followed by a slipped overhand knot on top, although the motor and visual patterns used to preserve the loops in the shoelaces differ from those associated with simply tying a generic composition of overhand knots: tying one trefoil after another without a loop. Analysis of the Ashley Book of Knots (1993) revealed that of the wide variety of knots containing granny and reef structures, the granny knot appears in 75% of cases (Scanlon, 2016). An analysis of impact in integrity of knot structure shows that the reef knot is less liable to come undone, suggesting that non-functional biases may be required to explain the prevalence of the granny over the reef forms (Grog; O'reilly et al., 2017).

Mathematically, a knot is a 3-dimensional closed curve, where the string is over and under itself in some way with the ends glued together. The left- and right-handed versions of the trefoil are mirror images of one another and are mathematically distinct as they cannot be transformed into each other by Reidemeister moves, a set of moves on the strands of a knot used to determine if two diagrams relate to the same knot (Reidemeister, 1927); the only way to change the left handed trefoil to the right handed trefoil is to cut the knot open and retie it. The granny and reef knots are distinct knots, and can be identified as such by knot invariants (Adams 2004; see Supplementary Material Section S1). The granny knots are distinct from each other and both reef knots, but the two reef knots are not distinct, which can be seen by rotating one reef knot to match the other; no such rotation is possible for the granny knots (Figure 1c).

Our study uses social transmission data to explore the interactive effects of learning processes on cultural evolutionary dynamics. We ran a social learning experiment whereupon participants were exposed to demonstration of one of the four composition of overhand knot variants and asked to copy the observed knot.

This generated data on the change in frequencies of the four knot variants across sequential generations of knot tyers. We then present a model that describes the non-linear, interactive effects of four putative learning processes (copying fidelity of the perceived demonstration, mirroring, handedness bias and repetition) on the change in the composition of overhand knot frequencies across sequential generations of knot tyers. We explore cultural evolutionary dynamics of the system before applying Approximate Bayesian Computation (ABC; Kandler and Powell 2018) to derive posterior estimates for the four learning processes. These estimates were used to predict evolutionary trajectories of the four knot variants which can then be compared against what we know of granny and reef knot frequencies in the wild.

Social Transmission Experiment

Participants were recruited from the student population of Durham University. They were rewarded with a £4 food voucher for their participation. In total 101 people took part in the experiment with 36 male. None of the participants were experts at learning to tie knots on command. Similar to adult learners in the wild who may attempt to copy the demonstration of the knot structure, the participants typically had some prior experience tying simple knots, although approximately two thirds claimed they did not know how to tie either a granny knot or a reef knot (see Section S3), and some even claimed to be unable to tie shoelaces.

The experiment took place in a lecture theatre, with batches of up to 10 participants at a time. We treated between-participant effects as independent by spacing participants widely across the lecture theatre and requiring each participant to tie their knots within a modified cardboard box which prevented between-participant observation.

For the social transmission experiment, participants were given a 35cm length of string and, using the overhead projector, shown a video demonstrating the tying of either a LL granny knot (26 participants), a RR granny knot (25 participants), a LR reef knot (25 participants) or a RL reef knot (25 participants), randomly assigned across batches. Screenshots of the video and the knots shown in Figure 1a clarify that the demonstrated knot was tied in its generic form, without the loops typically retained when tying shoelaces. Participants were instructed that the aim was to copy the knot shown in the video, which showed only hands tying a knot and contained no audio. The video was recorded from the point of view of an observer sitting opposite the demonstrator, so the observer would have to take the demonstrator's perspective to copy the correct knot handedness. Participants were shown the video three times, with a pause of 30 seconds between each showing.

They were told they could practice tying the knot whilst the video was being shown, and during the pauses between the showings. After the final showing of the video, they were told to untie any practice knots and to tie the knot shown in the video. Of the 101 knots tied after being shown the video, 100 of the knots were either LL, RR, LR or RL, and the remaining knot (a composition of the double overhand knot, 5_1 in the Alexander-Briggs notation, and the trefoil knot) was excluded from the analysis.

In additional exploratative analysis, described in Sections S2 and S3, we performed an asocial test of each participant's handedness bias run prior to the social learning experiment, and administered a short questionnaire after the social learning experiment requesting the participant's name, gender, degree programme, handedness, hand usually used for writing, and whether they knew how to tie a granny or reef knot.

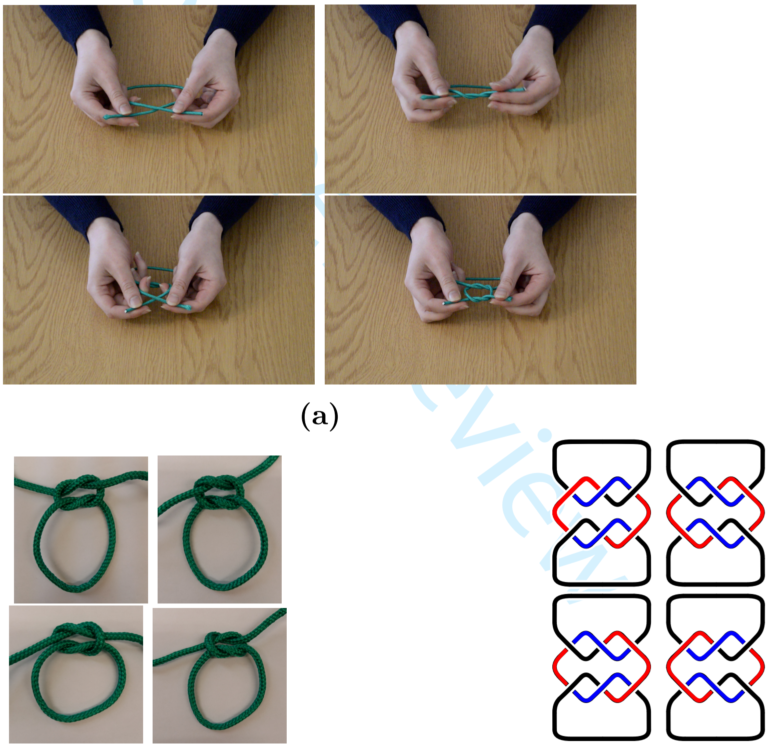

(a)

(b)

(c)

Figure 1. (a) Screenshots from a demonstration video used in the experiment, (b) tied versions of all four knots used, and (c) the four possible combinations of overhand knots depicted as 3-dimensional closed curves. Parts (b) and (c) both show top left: LL granny knot; top right: RR granny knot; bottom left: LR reef knot; bottom right: RL reef knot.

Table 1 indicates that participant behaviour in the social learning experiment was affected by the demonstration they observed. They were most likely to tie the knot shown in the video (the leading diagonal), but if a mistake was made, participants were most likely to tie the mirror image of the demonstrated knot over the other two variants. For example, more people tied the RR granny knot when shown LL, than tied either reef knot, LR or RL. Also, granny knots were more likely to be tied than reef knots, suggesting that participants may exhibit a bias to repeat the handedness of the first trefoil they tie. Finally, there was a very small bias towards left- over right-handed knots in the sample. See Section S4 for probability distributions of each knot being tied in response to a given demonstrated knot and for associations with trefoil handedness bias under asocial conditions (Section S2) and the questionnaire results (Section S3).

		Knot tied by participants				
		LL	RR	LR	RL	Total
Demonstration	LL	14	9	1	2	26
	RR	9	15	0	1	25
	LR	4	4	8	8	24
	RL	6	1	6	12	25
	Total	33	29	15	23	100

Table 1. Knots tied by participants given video shown in experiment, dashed lines delineate granny knots from reef knots

We suspect that multiple learning processes may be interacting to affect social transmission of the four variants so in the next section we identify four putative processes and specify in a model how they interact non-linearly to affect the social transmission of these knots. After exploring the cultural evolutionary properties of this model, we apply ABC to the experimental data, deriving posterior estimates and predicting evolutionary trajectories.

SOCIAL TRANSMISSION MODEL

Assumptions. We model the transmission of granny and reef knots within a population through oblique transmission (Cavalli-Sforza and Feldman, 1981) and assume a closed system such that when a granny or reef knot is demonstrated, the learned knot is always either a granny or a reef knot. We assume that four parameters can affect the fidelity of social transmission: the learner interprets the demonstrator's knot incorrectly as the knot's mirror image with a probability g (mirroring); the learner copies the perceived trefoil with a probability s (copying fidelity), where the perceived trefoil refers to the learner's interpretation of the demonstrated trefoil, which could either be the demonstrated knot or the mirror image of the demonstrated knot; the learner repeats the trefoil they tied for the first step of the composition of overhand knots with a probability r (repetition); and the learner ties a right-handed trefoil when they do not copy the perceived demonstration with a probability p (handedness).

Using these parameters, we can build a system of recurrence equations to describe relative knot frequencies in the learner generation as a function of their frequencies in the demonstrator generation. We denote the proportion of knot ij tied in the demonstrating generation by f_{ij} where $ij \in \{RR, LL, RL, LR\}$, and the knots tied by the learner generation of the population after transmission as f'_{ij} where $f'_{RR}+f'_{LL}+f'_{RL}+f'_{LR} = 1$ with each f'_{ij} taking values in the interval $[0,1]$. For example, take the granny knot formed by tying two right-handed trefoils and denote it by f_{RR}. This knot will be transmitted successfully if it is not mirrored and both trefoils that form it are accurately copied by the next generation, denoted by $f_{RR}(s^2(1-g))$. However, a right granny could also be formed by mirroring an LL with probability g and accurately copying both trefoils of the perceived knot with probability s^2, giving $f_{LL}(s^2 g)$. A right granny could also be formed with no copying fidelity at all ($s = 0$), if the learner has a bias towards tying right-handed trefoils $f_{RR}((1-s)^2 p^2)$ or repeating the first knot tied, $f_{RR}((1-s)^2(pr))$ and so we get the frequency of right granny knots in the population as a function of granny and reef knots already in the population and the probability parameters;

$$
\begin{aligned}
f'_{RR} = f_{RR}(s^2(1-g)) + \dots + f_{RR}((1-s)^2 p^2) + \dots \\
+ f_{RR}((1-s)^2(pr)) + \dots + f_{LL}(s^2 g) + \dots
\end{aligned}
\tag{1}
$$

It is important to think about how the parameters interact with each other. If a learner copies the knot correctly then the learner's likelihood to repeat or tie a right-handed trefoil does not matter. They will do what is shown regardless of their handedness bias or propensity for repetition, and so we can discount repetition and right-hand bias when the knot is accurately copied. In the same way, when the learner simply repeats part of a knot, their right-hand bias does not matter, as they will repeat regardless of this bias. So we can discount right-hand bias when repetition takes place. Figure 2 illustrates how the knot tied may be affected by the observed knot and the four parameters. Note that for each trefoil, the depicted order of parameters on any given branch is arbitrary and does not affect the probability that a particular trefoil form is tied (i.e. the parameters commute; see S5). For instance, the first trefoil can be tied left-handed if the learner both fails to copy the perceived knot and is not subject to a right-handedness bias irrespective of any order by which these processes might take effect. For each trefoil, the model only accounts for combinations of learning processes that lie on the same branch of the probability tree (see Discussion).

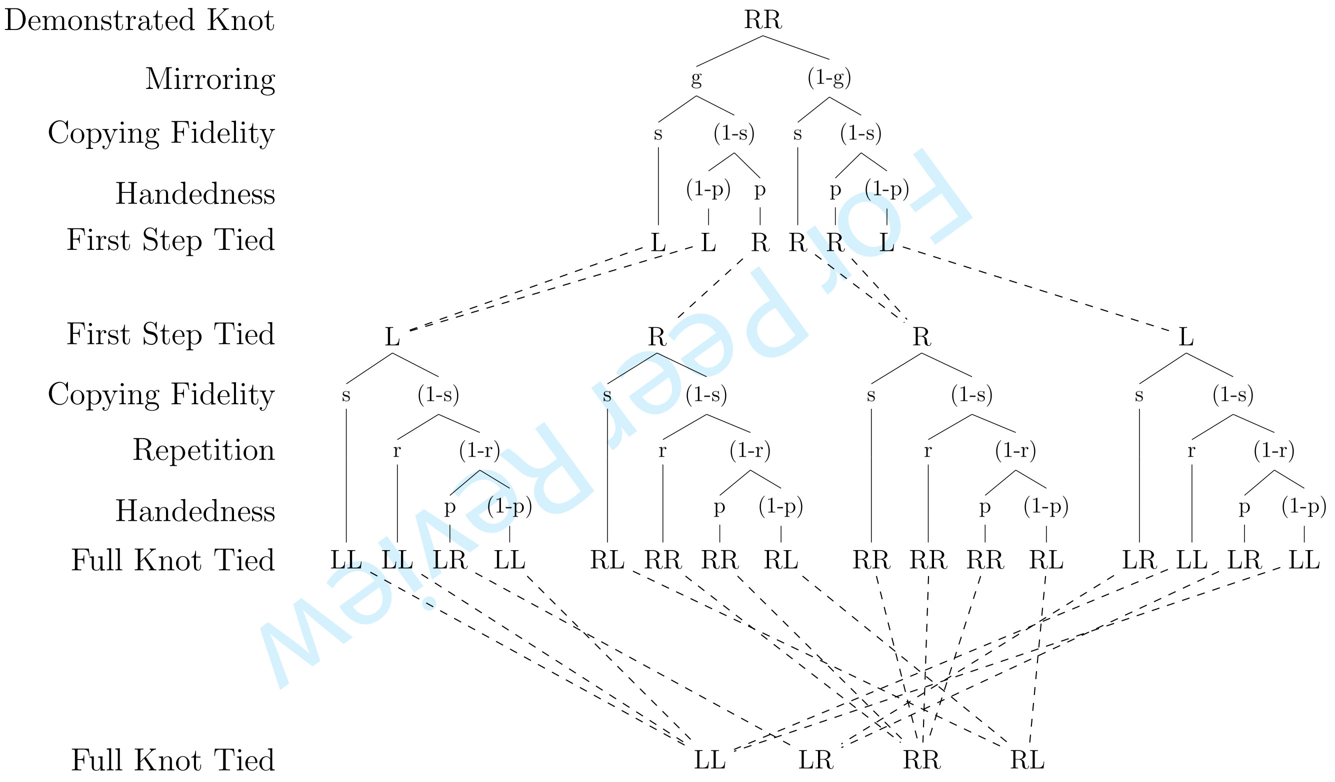

Figure 2. Probability tree showing the effect of parameters on the transmission of knot RR. For each trefoil tied, the order by which parameters is shown to take effect along a given branch is arbitrary as the probability that the knot is of form L or R is simply the product of their combined effect.

Evolutionary Dynamics. Each set of parameter values $0 \leq (s, g, r, p) \leq 1$, determines the evolutionary trajectory and a single equilibrium point, where $f_{ij} = f'_{ij} = \hat{f}_{ij}$, (expressions for equilibrium states are given in Appendix S6). If $s = 0$, the system jumps to a stable equilibrium point determined by the p and r and is unaffected by starting values of f_{ij}. By contrast, if copying is always accurate, $s = 1$, and mirroring never occurs, $g = 0$ $(0 \leq r \leq 1)$, the population does not evolve from starting frequencies, so if a small perturbation in frequencies is induced, the population remains at the new frequencies. If there is some copying, $0 < s < 1$, the population evolves to a stable equilibrium, such that the population returns to the original equilibrium state following a small perturbation in frequencies.

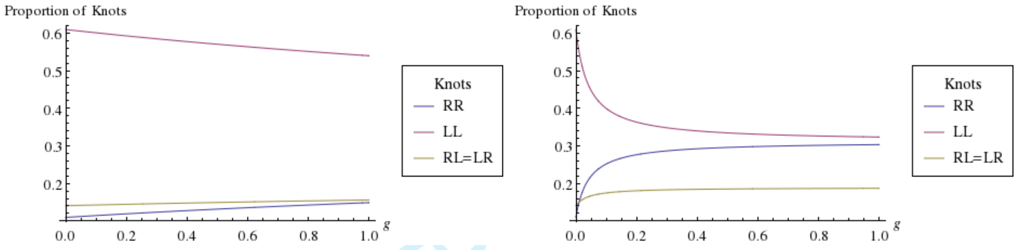

(a) p=0.25, r=0.25, s=0.1 (b) p=0.25, r=0.25, s=0.9

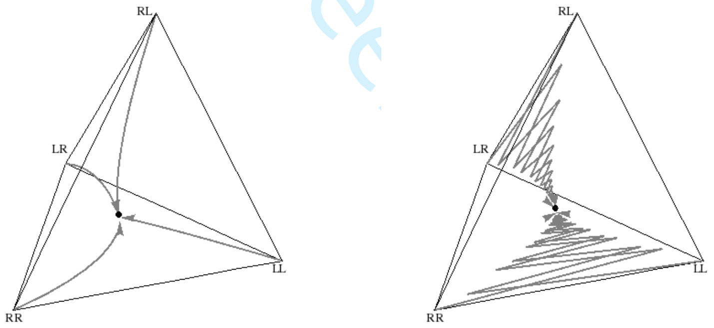

(c) p=0.75, g=0.1, r=0.25, s=0.9 (d) p=0.75, g=0.9, r=0.25, s=0.9

Figure 3. Parts 3a and 3b show the proportion of knots at equilibria as a function of the probability of mirroring when copying fidelity of the perceived knot is low and high, respectively. The values of $\hat{f}_{LR}$ and $\hat{f}_{RL}$ are equal so these are represented by the same line on the graph, while $\hat{f}_{RR}$ and $\hat{f}_{LL}$ are represented by separate lines. Parts 3c and 3d show evolutionary trajectories when the probability of mirroring is low and high, respectively. Each arrow represents the change in relative frequency of each type of knot in the population, starting from sole existence in each corner to a mixture of different knots in the interior of the tetrahedron. The solid disk is the equilibrium state which is evolved towards no matter the starting frequencies. Frequencies are plotted in tetrahedral space using Barycentric coordinates (see Appendix S8).

Figure 3 illustrates the effect of copying and mirroring on equilibrium frequencies. In Figure 3a, the value of s is set lower than in Figure 3b, resulting in a relatively small change in the values of $\hat{f}_{RR}$, $\hat{f}_{LL}$ and $\hat{f}_{RL}$ and $\hat{f}_{LR}$. This shows that copying needs to be highly probable for mirroring to affect the proportion of knots tied in the population. We notice that the two reef knot frequencies, f_{LR} and f_{RL}, are always equal at equilibria. This is consistent with the fact that LR and RL represent the same knot mathematically (see Section S1).

Prior to reaching an equilibrium state, evolutionary dynamics typically follow a smooth trajectory (assuming $0 < s < 1$), but a high probability of mirroring can cause oscillations in the trajectory when copying fidelity is high. When mirroring is low (Figure 3c), we see the system evolve in a smooth curve to a point strongly affected by the handedness, p and repetition, r. The high value of p causes the point to be slightly closer to the corner $f_{RR} = 1$ than $f_{LL} = 1$ but the low value of r does not cause the point to be as close to the $f_{RL} + f_{LR} = 1$ boundary as we may expect. In Figure 3d, mirroring is likely to occur. Coupled with the high copying fidelity, the system evolves to a similar equilibrium point as shown in Figure 3c, but the high probability of mirroring causes the path to oscillate to the point rather than evolve in a smooth trajectory.

Humans are likely to copy a perceived demonstration with some success but to make some mistakes. In this circumstance ($0 < s < 1$), there are some conditions where s does not affect equilibrium state frequencies.

If $p = \frac{1}{2}$, we have

$$\begin{aligned}\hat{f}_{RR} = \hat{f}_{LL} &= \frac{(1+r)}{4}\\ \hat{f}_{RL} = \hat{f}_{LR} &= \frac{(1-r)}{4}\end{aligned}$$

while if $g = 0$, we have

$$\begin{aligned}\hat{f}_{RR} &= p(p+r-pr)\\ \hat{f}_{LL} &= (1-p)(1-p+pr)\\ \hat{f}_{RL} = \hat{f}_{LR} &= (p-1)(pr-p)\end{aligned}$$

Most combinations of parameter values result in an excess of granny knots over reef knots at equilibrium. As noted above, any repetition, r, will favour the granny knot, but even when repetition never occurs, the population is still more likely to tie granny knots than reef knots if there is any handedness bias, $p \neq \frac{1}{2}$. Mirroring typically has little influence on the relative equilibrium frequency of granny to reef knots when $0 < s < 1$ and has no influence when either $s = 0$ or $s = 1$. Figure 4a illustrates the predominance of granny knots at equilibrium, taking the case where there is no repetition in the absence of guidance, $r = 0$, and intermediate mirroring, $g = \frac{1}{2}$. The bias towards granny knots is strongest when handedness bias, p, is either high or low and the copying coefficient, s, is low; in other words, when individuals consistently tie with the same handedness rather than copying a different knot.

Also note that the absence of non-random copying error does not lead to equal knot frequencies; granny knots are expected in higher frequency than reef knots (Figure 4b; also see that in Figure 5b the blue disc is not in the centre of the tetrahedron). This occurs because of the way the parameters interact to affect the knot forms: consider for instance the case in the absence of handedness bias and repetition bias $p = \frac{1}{2}, r = \frac{1}{2}$ (under these conditions, mirroring and copying fidelity do not affect equilibrium frequencies). Figure 4b shows that the probability of tying each knot is $P(LL) = \frac{3}{8}$ and $P(RR) = \frac{3}{8}$, and $P(RL) = \frac{1}{8}$ and $P(LR) = \frac{1}{8}$.

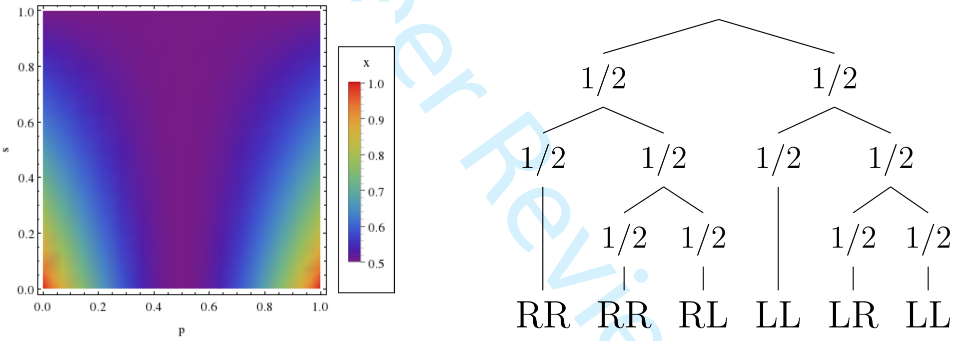

(a) (b)

Figure 4. Part (a) shows a density plots showing the proportion of granny knots at equilibrium, denoted by $x = \hat{f}_{RR} + \hat{f}_{LL}$, as a function of handedness bias, p and copying fidelity, s, where $g = \frac{1}{2}$ and $r = 0$. Part (b) shows a probability tree showing knots tied in the absence of biases in handedness ($p = \frac{1}{2}$; top two layers affecting first and second trefoil) and repetition biases ($r = \frac{1}{2}$; bottom layer, affecting second trefoil).

There are only two cases where the equilibrium proportion of granny and reef knots is equal ($\hat{f}_{RR} + \hat{f}_{LL} = \hat{f}_{RL} + \hat{f}_{LR}$). The first case is when copying is not perfect, $0 \leq s < 1$, the first knot is never repeated, $r = 0$, and there is no handedness bias, $p = \frac{1}{2}$, where $0 \leq g \leq 1$. The absence of repetition prevents predominance of granny knots, and the lack of handedness bias prevents the prevalence of either granny knot. The second case is when copying is perfect, $s = 1$, and there is some mirroring $0 < g \leq 1$, where $0 \leq p \leq 1$ and $0 \leq r \leq 1$. Here copying the perceived knot form is always perfect, but mirroring causes tying of the opposite handedness to that demonstrated. Both these cases are illustrated in Figure 4a. Finally, we note that reef knots can only be more prevalent than granny knots if this is exhibited in their starting frequencies and when the system does not evolve ($s = 1$ and $g = 0$; discussed above).

Fitting the Social Transmission Model to Experimental Data. Using Approximate Bayesian Computation (ABC; Sunnåker et al. 2013), we can use our model to estimate parameter values that predict the experimental data. ABC works on the same premise as Bayes' theorem, relating conditional probability of parameters θ, to data D by the rule

$$p(\theta|D) = \frac{p(D|\theta)p(\theta)}{p(D)}, \tag{2}$$

where $p(\theta|D)$ is referred to as the posterior, $p(\theta)$ represents the prior beliefs before any data is available, $p(D|\theta)$ the likelihood of data D occurring given the prior and $p(D)$ the evidence (Gelman et al., 2003). With this rule, we can calculate the posterior by taking the product of prior beliefs with the likelihood of data occurring, divided by the evidence observed. To obtain the probability of data D given parameter θ, we use our model to simulate data for a given parameter set and decide whether it fits the observed data. We construct a metric to describe our observed data such that we can accept or reject the simulated parameter set depending on whether it generated data within a tolerated proximity from the observed. The retained parameter distributions give us $p(\theta|D)$.

Taking our observed data from Table 1 as a 4×4 matrix O and simulating data of the same form using our model to give a 4×4 matrix S, we compare these two sets of data using the metric;

$$d(O, S) = \sum_{i,j} a_{ij}^2, \tag{3}$$

where a_{ij} are the entries of the matrix $O - S$. This metric is proportional to finding the Euclidean distance between the points in the two matrices.

Describing the process in more detail, we ran a Monte Carlo simulation (Hastings, 1970) where the number of simulated learners exposed to each of the four demonstrated knots matched the number of participants in each experimental condition (see Table 1). A value for each of the four parameters (p, g, r, s) was sampled from a uniform distribution between zero and one. The knot tied by each simulated learner was derived by walking through the relevant probability tree with a Bernoulli trial at each internal node (e.g. Figure 2 for a learner that observes demonstration of knot RR). This simulation procedure was repeated many times to build up parameter distributions for all the simulations that resulted in a metric value, $d(O, S) = \sum_{i,j} a_{ij}^2 \leq 0.0075$, coming from fewer than 0.5% of the simulations.

Figure 5a shows uncertainty in handedness bias, with a broad distribution around a mean of $\bar{p} = 0.5$ $(sd = 0.28)$ which is where handedness bias is absent. The model predicts that individuals mirror fairly frequently $(\bar{g} = 0.39, sd = 0.07)$ but that knots are mirrored less often than they are correctly interpreted. There is uncertainty in the posterior estimate of the repetition bias, but with a trend to be more likely to repeat the handedness of the first trefoil tied than not $(\bar{r} = 0.66, sd = 0.24)$. Finally, there is relatively high copying fidelity of the perceived knot $(\bar{s} = 0.81, sd = 0.08)$.

We can establish what effect our parameter estimates would have on the cultural evolution of granny and reef knots by plugging the central tendency values into the model. For illustration, we use the mean from each posterior parameter distribution, but note that sampling from the posterior distributions each generation gives similar results (see Section S11.)

Figure 5b illustrates how the population evolves towards a single polymorphic equilibrium state, no matter the starting distribution (grey arrows leading to black disc). Compared to the case where handedness and repetition errors are random $(p = \frac{1}{2}, r = \frac{1}{2}$; blue arrows leading to blue disc), the mean posterior estimate of repetition bias results in a higher equilibrium frequency of granny over reef knots. The mean posterior estimate for the handedness coefficient is unbiased, $\bar{p} = \frac{1}{2}$, resulting in the equal equilibrium frequency of left and right forms of granny knot. As established in the social transmission model analysis, the posterior copying fidelity value, $\bar{s} = 0.81$ actually has no effect on the equilibrium frequencies when there is no handedness bias. The posterior mirroring value is not large enough to cause the characteristic oscillating dynamics shown in Figure 3d. We see that the equilibrium frequency results in a prevalence of granny knots over reef which can also be explored by sampling from the posterior distribution of parameter values, allowing us to see the relative frequency of granny knots over reef knots for one generation (see Section S12.)

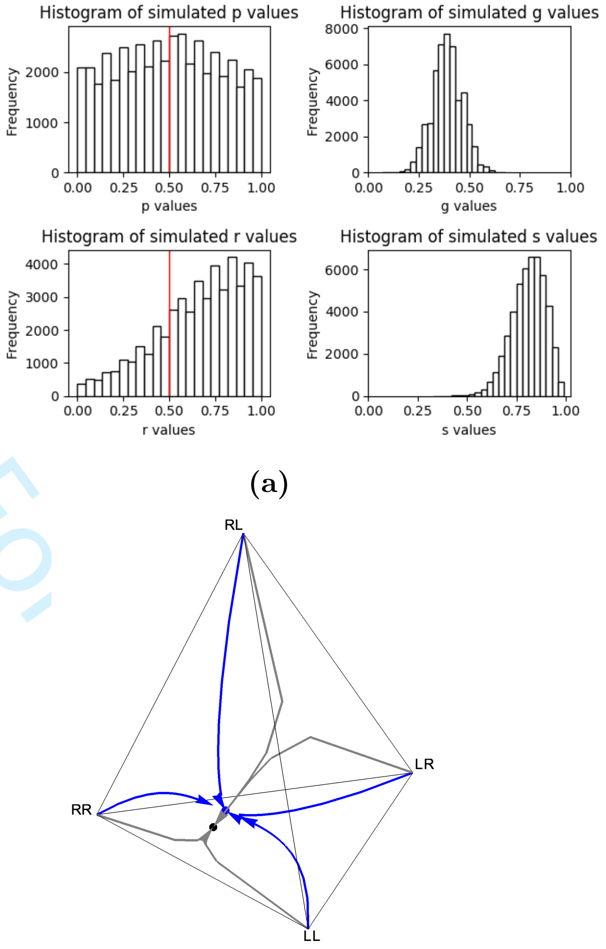

(a)

(b)

Figure 5. Part (a) shows histograms of parameter values simulated from experiment, with acceptance interval $d(O, S) \leq 0.0075$. Red lines indicate unbiased parameter values, $p = \frac{1}{2}$ and $r = \frac{1}{2}$, giving equal probability of tying right- and left-handed trefoils and equal probability of repeating the previous knot as not, respectively. Part (b) shows evolutionary trajectories of the four knot forms, where $f_{ij} = 1$ in each corner and frequencies are equal at the centre of the tetrahedron. Trajectories using the mean posterior parameter values $(\bar{s}, \bar{p}, \bar{g}, \bar{r})$ are shown by the grey arrows and black disc, $\hat{f}_{LL} = \hat{f}_{RR} = 0.415$, $\hat{f}_{LR} = \hat{f}_{RL} = 0.085$. The blue arrows and disc, $\hat{f}_{LL} = 0.375$, $\hat{f}_{RR} = 0.375$, $\hat{f}_{LR} = \hat{f}_{RL} = 0.125$, show the trajectories in the absence of handedness bias and repetition bias $(p = \frac{1}{2}, r = \frac{1}{2})$ assuming no mirroring, $g = 0$, and the mean posterior parameter value for copying fidelity, $\bar{s} = 0.81$ (note that mirroring and copying fidelity do not affect the equilibrium state here).

As an aside, in Section S9 we compare our social transmission model against a non-parametric estimate of equilibrium frequencies which can be found simply by iterating this proportional change without specifying the effects of specified learning processes (Claidière et al., 2014). Our parametric social transmission model results in similar equilibrium frequencies to this non-parametric prediction, indicating that the close match in the proportional change in knot frequencies over one social transmission episode caused by implementing ABC is preserved over multiple generations.

A comprehensive out-of-sample test of the model is for a future study, although we note that, for composite knots within the Ashley corpus, the proportion of granny to reef knots exactly matches the 3 to 1 ratio predicted by the equillibrium state of our model when handedness and repetition errors are random ($p = 0.5, r = 0.5$; blue disk in Figure 5b) and is fairly similar to that predicted using the posterior parameter estimates (mean posterior estimates give 83% granny knots; black disk in Figure 5b) (Ashley, 1993; Scanlon, 2016)).

DISCUSSION

Our results suggest that participants exhibited a tendency for repetition and had approximately a one-in-five chance of failing to faithfully reproduce the perceived trefoil, which was sometimes the mirror image of the demonstrated knot. There was no clear handedness bias although the posterior exhibited considerable uncertainty. Our model predicts that a population expressing these posterior estimates would evolve towards an equilibrium characterised by a preponderance of granny knots over reef knots. Exploration of the model contextualises this finding to show that the prevalence of granny over reef knots is to be expected across most of parameter space, including in the absence of handedness and repetition biases. These results are consistent with empirical evidence for a prevalence of granny over reef knots found in Ashley's collection. Our results show that this pattern may not necessarily be caused by a preference for granny over reef knots, but may simply be the outcome of copying error processes affecting the construction of the knots.

ABC is a useful inductive tool to estimate the probabilistic effects of distinct putative learning processes that interact in ways specified by a social transmission model (Kandler and Powell, 2018). The model can be used both to understand how learning processes can affect cultural evolutionary dynamics and to predict evolutionary trajectories based on posterior estimates. The strong copying fidelity of the perceived knot suggests that the demonstrated knot affected participant behaviour, yet analysis of the model shows that this fidelity will not affect equilibrium frequencies in the absence of a handedness bias: there was large uncertainty over the handedness posterior estimate with only a very weak unbiased central tendency which would result in evolution towards parity of left- and right-handed knots. The effect of mirroring on evolutionary dynamics is contingent on copying fidelity of the perceived knot. Our posterior mirroring estimate suggests that faithful cultural transmission of bilaterally symmetrical tasks can be vulnerable to the correspondence problem (Heyes and Bird, 2007). Our experimental setup had learners sitting opposite the demonstrator's perspective and so our posterior mirroring value provides an estimate of the maximum mirroring effect, presuming that learners may be less vulnerable to this error if they were to sit side-by-side, taking a similar visual perspective. Nonetheless, our analysis indicates that mirroring typically has little effect on the relative equilibrium frequencies of granny and reef knots. The repetition posterior estimate exhibited considerable uncertainty but with a trend towards high values. While complex skills can be honed by repetition, a tendency for inadvertent repetition of an action can reduce within-sequence variation over cultural generations, in this case promoting granny over reef knots, and that even a small repetition bias can have a substantial effect on evolutionary dynamics within our system.

The participants' response to the task, reflected in the posterior distributions, is likely to have been shaped by genetic and cultural influences, including experience tying either a trefoil or a composition of them. Future studies can establish the generality of these posterior estimates and the relevance of the predicted evolutionary trajectories, both for these compositions of overhand knots and for overhand knot structures within more complex knots. Similarity between the equilibrium state predictions and the relative frequencies of granny and reef knots in the Ashley corpus provides some support for the model's out-of-sample performance, although it is not clear that Ashley's depiction of handedness in composite knot forms accurately reflects their relative frequencies in the wild. Nonetheless, our model helps to explain the apparent prevalence of granny over reef knots when functional investigation suggests that the reef knot is superior (Grog; O'reilly et al., 2017).

Under some conditions, the model behaviour contradicts the common assertion that population-level homogeneity is a signature of high copy fidelity. If there is a handedness bias or propensity for repetition, our system exhibits greater homogeneity (a preponderance of granny knots) at equilibrium when copying fidelity is low than when it is high: low copying fidelity allows the handedness and repetition to take effect, reducing heterogeneity. Thus population-level measures of cultural variation are not necessarily accurate proxies of between-individual learning processes (Acerbi et al. (2016), but see Smaldino et al. (2018) and Acerbi et al. (2018)). Copying fidelity in our model is of the demonstrated knot as perceived by the learner and so a copying fidelity of $s = 1$ can still result in an error if there is mirroring. Nonetheless, when there is a bias in handedness or a propensity for repetition, the relationship between copying fidelity and heterogeneity at equilibrium holds as mirroring typically has little effect the relative equilibrium frequencies of granny and reef knots.

More generally, imperfect copying encourages the evolution of heterogeneity when there is a closed set of alternative behaviours and failure to copy one variant results in adoption of another (see Section S10). This mechanism is responsible for the model's prediction that the two reef knot forms will evolve towards equal frequencies; note there is no assumption that individuals recognise both forms of reef knot to be mathematically indistinct. Mirroring also pushes the population toward equal frequencies of knot forms because it is most likely, by chance, to reverse the handedness of the most common trefoil.

Future work can explore conditional relations between the learning processes by comparing explanatory value of alternative putative conditional rules through model selection. Rules such as copy the perceived trefoil only if there is no handedness bias would would require a new model as, for each trefoil, the copying parameter s lies on a different branch of the tree from the absence of handedness effect, $(1 - p)$ (see Figure 2). It will also be valuable to incorporate effects of perceived functionality and social value associated with knot structures in future analysis. Evolvability of complex knots within design space may be particularly susceptible to copying error biases where variation in knot structure is redundant in relation to practical or social function.

Commenting on the utility of evolutionary approaches to study patterns of artefact variation, Lycett (2015, pg. 27) states that "some of the most key advances in evolutionary approaches over the coming years are likely to center on increased empirical understanding of the links between processes of transmission and resultant artefactual variation, and moreover, the types of behavioural factors that influence patterns of variation in particular ways". To this end, our study provides statistical evidence that putative learning processes interact to affect cultural evolutionary dynamics of bilaterally-symmetrical artefact production. Our experimental and theoretical simulations of social transmission can be complimented both by controlled experiments to uncover proximal cognitive mechanisms underpinning the identified statistical profile, and by ethnographic accounts of social and functional value including group identity, aesthetic appeal and pedagogical norms scaffolding transmission.

End Section Statements

Acknowledgements. We thank Anne Kandler and Dirk Schuetz for insightful comments on an early draft, Thom Scott-Phillips for discussion of the non-parametric modelling approach, and the Spock team for participating in a pilot study. We thank the editor and reviewer for their helpful comments.

Author Contributions. LAS, AL, JJT and JRK designed the study. LAS carried out the analysis. LAS, AL, JJT and JRK wrote the manuscript. All authors gave final approval for publication.

Funding. The project was supported by the Leverhulme Trust grant awarded jointly to Durham University and Bristol University on The Scientific Properties of Complex Knots (SPOCK).

Ethics. The authors assert that all procedures contributing to this work comply with the ethical standards of the relevant national and institutional committees on human experimentation and with the Helsinki Declaration of 1975, as revised in 2008.

Conflicts of Interest. LAS, AL, JJT and JRK declare none.

Data Accessibility. Data are available from the Open Science Framework: https://doi.org/10.17605/OSF.IO/GZ2PS

REFERENCES

Alberto Acerbi, Edwin J.C. Van Leeuwen, Daniel B.M. Haun, and Claudio Tennie. Conformity cannot be identified based on population-level signatures. *Sci. Rep.*, 6(1):36068, dec 2016. ISSN 20452322. doi: 10.1038/srep36068.

Alberto Acerbi, Edwin J.C. Van Leeuwen, Daniel B.M. Haun, and Claudio Tennie. Reply to Sigmoidal Acquisition Curves are Good Indicators of Conformist Transmission. *Sci. Rep.*, 8(14016), Sept 2018. doi: 10.1038/s41598-018-30382-0.

Colin C Adams. *The Knot Book: An Elementary Introduction to the Mathematical Theory of Knots.* American Mathematical Soc., 2004.

Clifford W Ashley. *Ashley Book of Knots.* Faber and Faber Limited, 1993.

Luigi Luca Cavalli-Sforza and Marcus W Feldman. *Cultural Transmission and Evolution: A Quantitative Approach.* Princeton University Press, 1981. ISBN 0691082839.

Nicolas Claidière, Thomas C Scott-Phillips, and Dan Sperber. How Darwinian is cultural evolution? *Philos. Trans. R. Soc. B Biol. Sci.*, (March), 2014.

Jelmer W Eerkens and Carl P Lipo. Cultural transmission, copying errors, and the generation of variation in material culture and the archaeological record. *J. Anthr. Archaeol.*, 24(4):316–334, 2005. ISSN 02784165. doi: 10.1016/j.jaa.2005.08.001.

Andrew Gelman, John B Carlin, Hal S Stern, and Donald B Rubin. *Bayesian Data Analysis*, volume 2. Chapman and Hall/CRC, 3 edition, 2003. ISBN 158488388X. doi: 10.1017/CBO9781107415324.004.

Grog. Animated Knots: How to tie the Reef Knot. URL `http://www.animatedknots.com/reef/`.

Marcus J Hamilton and B Buchanan. The accumulation of stochastic copying errors causes drift in culturally transmitted technologies: Quantifying clovis evolutionary dynamics. *Journal of Anthropological Archaeology*, 28:55–69, 2009.

W. K. Hastings. Monte carlo sampling methods using Markov chains and their applications. *Biometrika*, 57(1):97–109, apr 1970. ISSN 00063444. doi: 10.1093/biomet/57.1.97.

Cecilia Heyes and Geoffrey Bird. Mirroring, association, and the correspondence problem. *Sensorimotor Found. High. Cogn.*, pages 461–480, 2007. doi: 10.1093/acprof:oso/9780199231447.003.0021.

Anne Kandler and Adam Powell. Generative inference for cultural evolution. *Philosophical Transactions of the Royal Society B Biological Sciences*, 373(1743), 2018.

Marius Kempe, Stephen Lycett, and Alex Mesoudi. An Experimental Test of the Accumulated Copying Error Model of Cultural Mutation for Acheulean Handaxe Size. *PLoS One*, 7(11), 2012. ISSN 19326203. doi: 10.1371/journal.pone.0048333.

Kevin N Laland, Jochen Kumm, John D Van Horn, and Marcus W Feldman. A gene-culture model of human handedness. *Behav. Genet.*, 25(5):433–445, sep 1995. ISSN 00018244. doi: 10.1007/BF02253372. URL `http://www.ncbi.nlm.nih.gov/pubmed/7487840`.

Stephen J. Lycett. Cultural evolutionary approaches to artifact variation over time and space: basis, progress, and prospects. *Journal of Archaeological Science*, 56: 21–31, 2015.

Oliver M O'reilly, Christopher A Daily-Diamond, and Christine E Gregg. The roles of impact and inertia in the failure of a shoelace knot. *Proc. R. Soc. A Math. Phys. Eng. Sci.*, 2017. ISSN 1364-5021. doi: 10.1098/rspa.2016.0770.

Kurt Reidemeister. Elementare Begründung der Knotentheorie. *Abhandlungen aus dem Math. Semin. der Univ. Hambg.*, 5(1):24–32, dec 1927. ISSN 0025-5858. doi: 10.1007/BF02952507.

L A Scanlon. Study of knots in material culture. *J. Knot Theory Ramifications*, 25(9), 2016. ISSN 02182165. doi: 10.1142/S0218216516410157.

Paul E. Smaldino, Lucy M. Aplin, and Damien R. Farine. Sigmoidal Acquisition Curves Are Good Indicators of Conformist Transmission. *Sci. Rep.*, 8(14015), Sept 2018. doi: 10.1038/s41598-018-30248-5.

Mikael Sunnåker, Alberto Giovanni Busetto, Elina Numminen, Jukka Corander, Matthieu Foll, and Christophe Dessimoz. Approximate Bayesian Computation. *PLoS Comput. Biol.*, 9(1):e1002803, jan 2013. ISSN 1553734X. doi: 10.1371/journal.pcbi.1002803.

Gerre Van der Kleij. On Knots and Swamps: Knots in European Prehistory. In J.C. Turner and P. C. Van de Griend, editors, *Hist. Sci. Knots*, pages 31–42. World Scientific, 1998.

Charles Warner and Robert G Bednarik. Pleistocene Knotting. In P C Turner, J.C. Van de Griend, editor, *Hist. Sci. Knots*, pages 3–18. World Scientific, 1998.

SUPPLEMENTARY MATERIAL: UNKNOTTING THE INTERACTIVE EFFECTS OF LEARNING PROCESSES ON CULTURAL EVOLUTIONARY DYNAMICS

LAUREN A. SCANLON[1,2], ANDREW LOBB[1], JAMSHID J. TEHRANI[2], JEREMY R. KENDAL[2]
[1]DEPARTMENT OF MATHEMATICS, DURHAM UNIVERSITY
[2]DEPARTMENT OF ANTHROPOLOGY AND DURHAM CULTURAL EVOLUTION RESEARCH CENTRE, DURHAM UNIVERSITY
CORRESPONDENCE EMAIL: JEREMY.KENDAL@DURHAM.AC.UK

S1. Knot Invariants

Knot invariants will give the same result when two knots are the same, and different results when they are distinct. The Jones polynomial Jones (1985), denoted $V(t)$, is one such invariant, which assigns a Laurent polynomial with integer coefficients in one variable $t^{1/2}$ to each knot and gives us some information about the crossings of that knot. The Jones polynomial is given for the left-handed granny knot in Equation S1, the right-handed granny knot in Equation S2 and both reef knots by Equation S3. We can see that the Jones polynomial for the left-handed granny knot differs from the right-handed granny knot by the sign of the exponents in the polynomial, the exponents for the left-handed granny knot are all negative whilst they are positive for the right-handed granny knot. This is the only difference between the two polynomials and shows that the left-handed and right-handed granny knot are mirror images of one another. Both versions of the reef knot have the same Jones polynomial which contains both positive and negative values for the exponents showing that there is no difference between the two versions of this knot. These polynomials show that the granny knots are distinct from each other and both reef knots, but the two reef knots are not distinct, which can be seen by rotating one reef knot to match the other; no such rotation is possible for the granny knots (See Figure 1c).

$$V_{LL}(t) = t^{-2} + 2t^{-4} - 2t^{-5} + t^{-6} - 2t^{-7} + t^{-8} \tag{S1}$$

$$V_{RR}(t) = t^{2} + 2t^{4} - 2t^{5} + t^{6} - 2t^{7} + t^{8} \tag{S2}$$

$$V_{reef}(t) = -t^{3} + t^{2} - t + 3 - t^{-1} + t^{-2} - t^{-3} \tag{S3}$$

S2. Asocial Handedness Bias Experiment

We asked participants to tie a "simple knot". We then checked that this was a trefoil knot. The knot was undone, then participants were asked to tie a "simple knot" every 60s over a 10 minute period. Each knot was tied in a separate 25cm length of string and the sealed in a small plastic bag. Over the same period, participants were asked to complete a distraction task in between tying each knot, requiring them to draw six concepts in order that another person could match the concepts to the drawings at a later time. Both the plastic bag containing the 10 knots and the paper with the drawings from the distraction task were collected in at the end of this stage.

For each participant, we recorded knot handedness over the 10 trefoils as an estimate of knot handedness bias in the absence of a demonstration. The frequency of right-handed trefoils tied by each person is shown in Figure S1, where participants who tied no right-handed trefoils tied all left-handed trefoils. Two participants tied knots that were not trefoils and have not been included in these data.

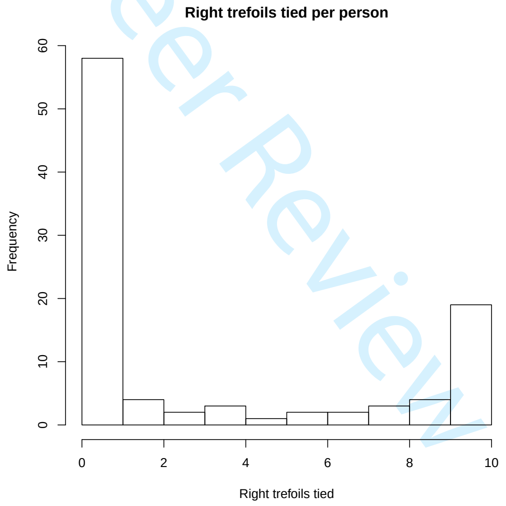

Figure S1. Frequency of right-handed trefoils tied by participants, those who tied no right-handed tied all left-handed trefoils and vice versa

The majority of participants tied either all right-handed or all left-handed trefoils, with a few tying a mixture of the two. Left-handed trefoils were much more common than right-handed trefoils. The mean proportion of right-handed trefoils tied per person was 0.32. This asocial handedness bias is compared against the handedness bias estimate derived from the social transmission experiment. See Section S4) for weak evidence that individuals who typically write with their right hand were more likely to tie a left-handed trefoil than those who write with their left, while those using their left hand to write were more likely to tie a right-handed trefoil than those who use their right. This weak evidence agrees with Chisnall (2010) who, through a survey involving the tying of multiple knots including trefoil knots and shoelace knots, found right handers tied a higher proportion of left handed knots than left handers and visa versa.

We note some association between the asocial handedness bias and the first knot tied by participants in the social transmission experiment (Table S1).

		Social trans. expt. knots tied				
		LL	RR	LR	RL	Total
Asocial handedness bias	Left	25	20	12	11	68
	Right	6	9	2	12	29
	Total	31	29	14	23	97

Table S1. Knot frequencies in the social transmission experiment given handedness of trefoil previously tied by the same participants under asocial conditions; dashed lines delineate granny knots from reef knots.

S3. Questionnaire Information

Participants were asked to complete a questionnaire detailing their name, gender, degree programme, handedness and hand usually written with and whether they knew how to tie a reef or granny knot. The questionnaire was filled in by participants at the end of the experiment, when all materials had been collected.

		Trefoil Tied		
		Right	Left	Total
Hand usually written with	Right	25	62	87
	Left	4	6	10
Self-reported handedness	Right	23	58	81
	Left	4	5	9
	Ambidextrous	2	5	7
	Total	29	68	97

Table S2. Handedness of trefoils tied given hand usually written with.

The majority of participants usually wrote with their right hand and tied a majority of left-handed trefoils. Using Bayesian association analysis (Gelman et al., 2003; Bååth, 2014) shown in Figure S2 we see there is weak evidence for a larger probability of tying a left-handed trefoil than right-handed trefoil by participants who usually wrote with their right hand than those who wrote with their left. Similarly there is weak evidence for a larger probability of tying a right-handed trefoil than left-handed trefoil by those who usually wrote with their left hand. However, the proportion of participants who usually wrote with their left hand is quite low so might not be wholly representative. A similar result can be found using the self reported handedness data with those reporting as ambidextrous having a larger probability of tying a left- than a right-handed trefoil. Acknowledging the small sample size, most of those reporting as ambidextrous usually wrote with their right hand which fits with the test of proportions for hand written with and trefoil tied.

Participants were asked to record their gender in a free-form box.

		Tied correct knot		
		Y	N	Total
Gender	Male	19	17	36
	Female	28	33	61
	Other	2	1	3
	Total	49	51	100

Table S3. Performance in experiment given gender

Table S3 shows the proportion of participants who tied the knot shown in the video given their gender. It is clear to see that gender had no bearing on their performance in the experiment.

Participants were also asked whether they knew how to tie a granny and a reef knot.

		Knot tied		
		Granny	Reef	Total
Knew how to tie a granny knot	Yes	17	13	30
	No	45	25	70
	Total	62	38	100

Table S4. Performance in experiment given knowledge of granny knots

		Knot tied		
		Granny	Reef	Total
Knew how to tie a reef knot	Yes	17	17	34
	No	45	21	66
	Total	62	38	100

Table S5. Performance in experiment given knowledge of reef knots

Tables S4 and S5 show the proportion of participants who tied granny and reef knots given the self-reported knowledge. Approximately one third of participants reported that they knew how to tie each knot. There is weak evidence that overall bias towards granny knots over reef knots is stronger in those that self-reported that they did not know how to tie these knots than those that did.

S4. Association Analysis

Posterior simulations of the test of proportions generated using R package Bayesian First Aid (Bååth, 2014). The test of proportions assumes flat priors constructed as a Beta(1,1) distribution.

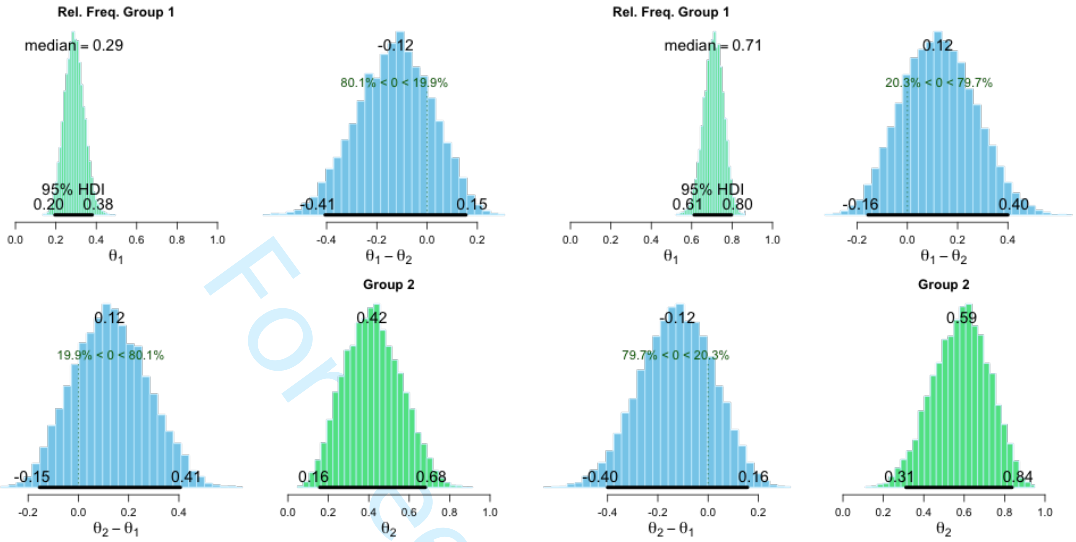

(a) Posterior simulation of right trefoils tied (b) Posterior simulation of left trefoils tied

Figure S2. Figure S2a shows the posterior simulations of tying a right handed trefoil by those who wrote with a specified hand. θ_1 refers to those who wrote with their right hand and tied a right trefoil whilst θ_2 refers to those who wrote with their left hand and tied a right trefoil. The differences $\theta_1 - \theta_2$ and $\theta_2 - \theta_1$ refer to the difference between these groups. There is weak evidence that a larger probability of those who write with their left hand tie a right handed trefoil than those who wrote with their right hand. Figure S2b shows the posterior simulations of tying left handed trefoils by those who wrote with either hand. θ_1 refers to those who wrote with their right hand and tied a left trefoil whilst θ_2 refers to those who wrote with their left hand and tied a left trefoil. The differences $\theta_1 - \theta_2$ and $\theta_2 - \theta_1$ refer to the difference between these groups. There is weak evidence that a larger probability of those who write with their right hand tie a left handed trefoil than those who wrote with their left hand. If we look at both Figures S2a and S2b we see those who wrote with their right hand were more likely to tie a left- than a right-handed trefoil. Those who wrote with their left hand were slightly more likely to tie a left handed trefoil than a right handed as the left handed trefoil was the most common amongst both groups and there were relatively few people reporting as writing with their left hand.

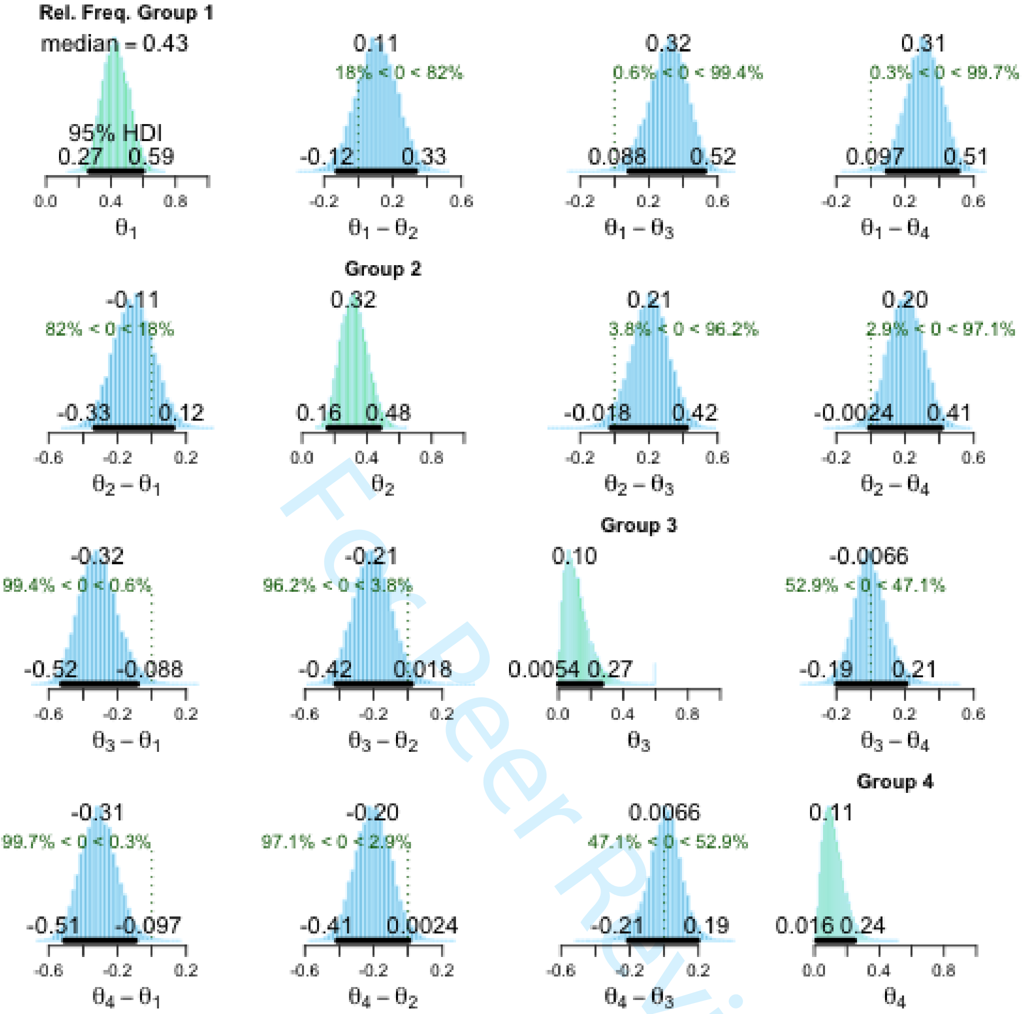

Figure S3. Posterior simulation of LL knots tied given demonstration knot. θ_1 refers to those who were shown the knot LL and tied LL, θ_2 those who were shown RR and tied LL, θ_3 those who were shown LR and tied LL and θ_4 those who were shown RL and tied LL with $\theta_i - \theta_j, (i, j \in \{1, 2, 3, 4\}, i \neq j)$ referring to the difference between groups. We see a larger probability for those who were shown either LL or RR tying LL than LR or RL, with those shown LL having the largest probability.

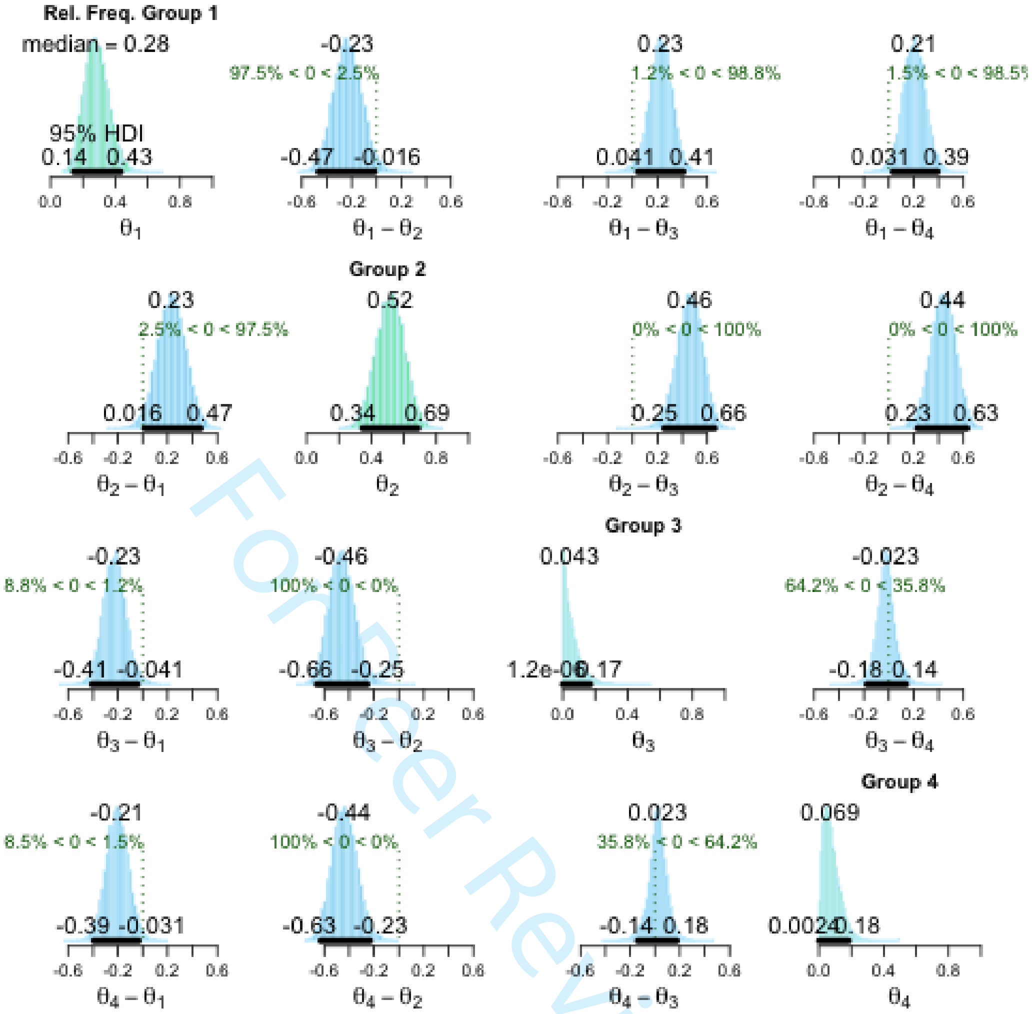

Figure S4. Posterior simulation of RR knots tied given demonstration knot. θ_1 refers to those who were shown the knot LL and tied RR, θ_2 those who were shown RR and tied RR, θ_3 those who were shown LR and tied RR and θ_4 those who were shown RL and tied RR with $\theta_i - \theta_j, (i, j \in \{1, 2, 3, 4\}, i \neq j)$ referring to the difference between groups. We see a larger probability for those who were shown either LL or RR tying RR than LR or RL, with those shown RR having the largest probability.

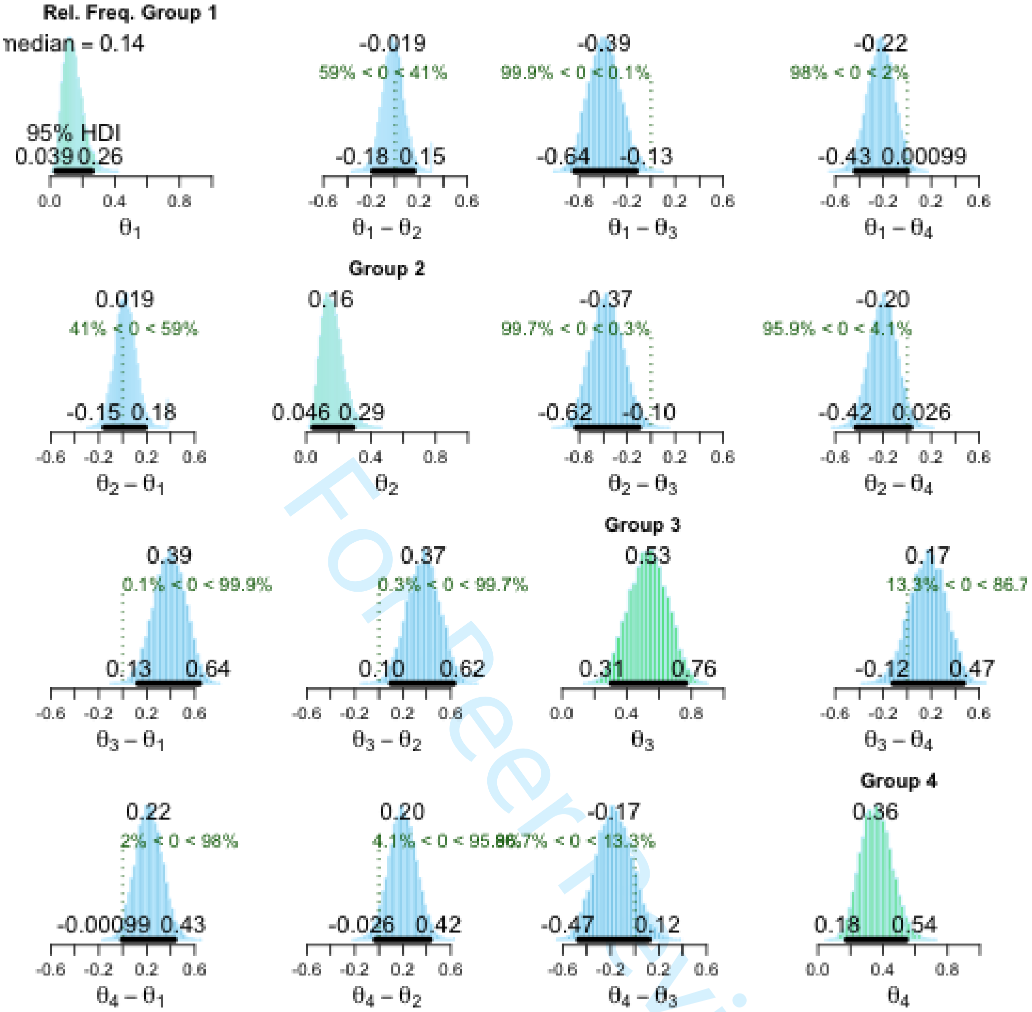

Figure S5. Posterior simulation of LR knots tied given demonstration knot. θ_1 refers to those who were shown the knot LL and tied LR, θ_2 those who were shown RR and tied LR, θ_3 those who were shown LR and tied LR and θ_4 those who were shown RL and tied LR with $\theta_i - \theta_j, (i, j \in \{1, 2, 3, 4\}, i \neq j)$ referring to the difference between groups. We see a larger probability for those who were shown either LR or RL tying LR than LL or RR, with those shown LR having the largest probability.

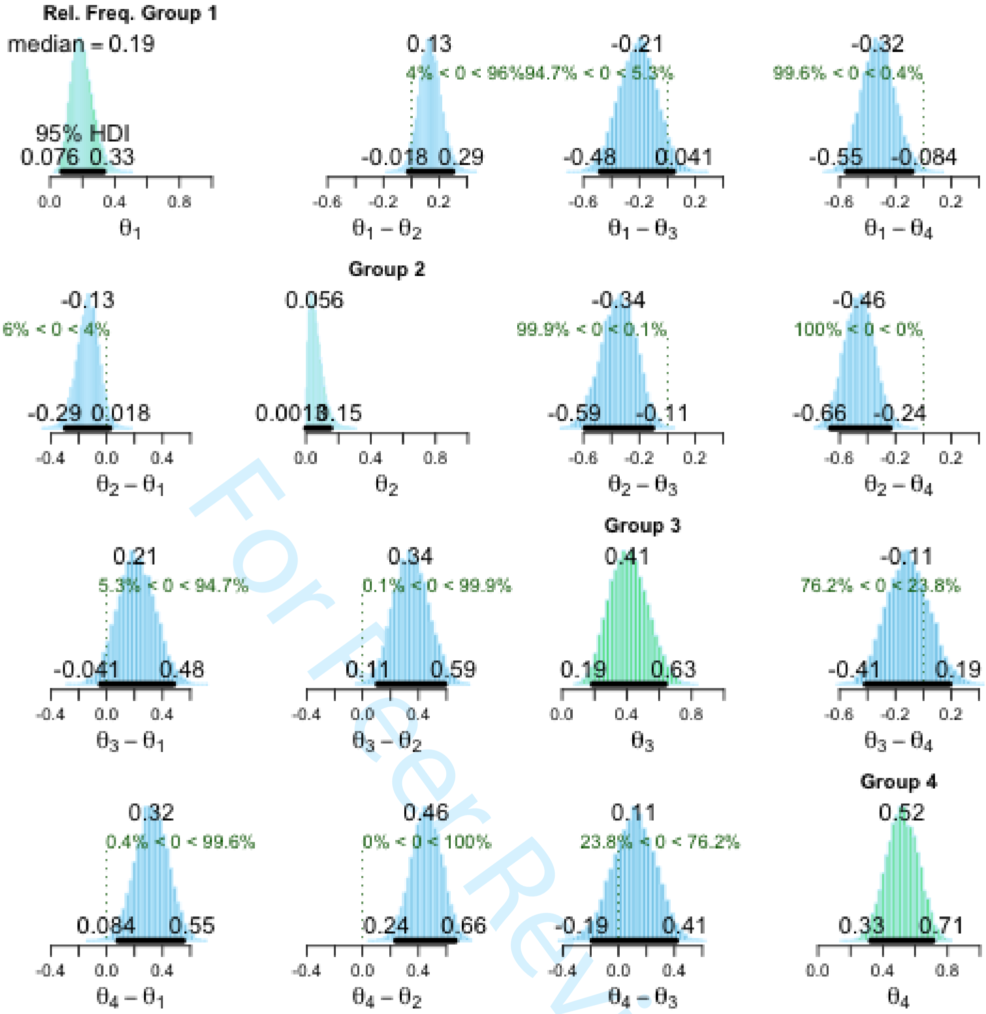

Figure S6. Posterior simulation of RL knots tied given demonstration knot. θ_1 refers to those who were shown the knot LL and tied RL, θ_2 those who were shown RR and tied RL, θ_3 those who were shown LR and tied RL and θ_4 those who were shown RL and tied RL with $\theta_i - \theta_j, (i, j \in \{1, 2, 3, 4\}, i \neq j)$ referring to the difference between groups. We see a larger probability for those who were shown either LR or RL tying RL than LL or RR, with those shown RL having the largest probability.

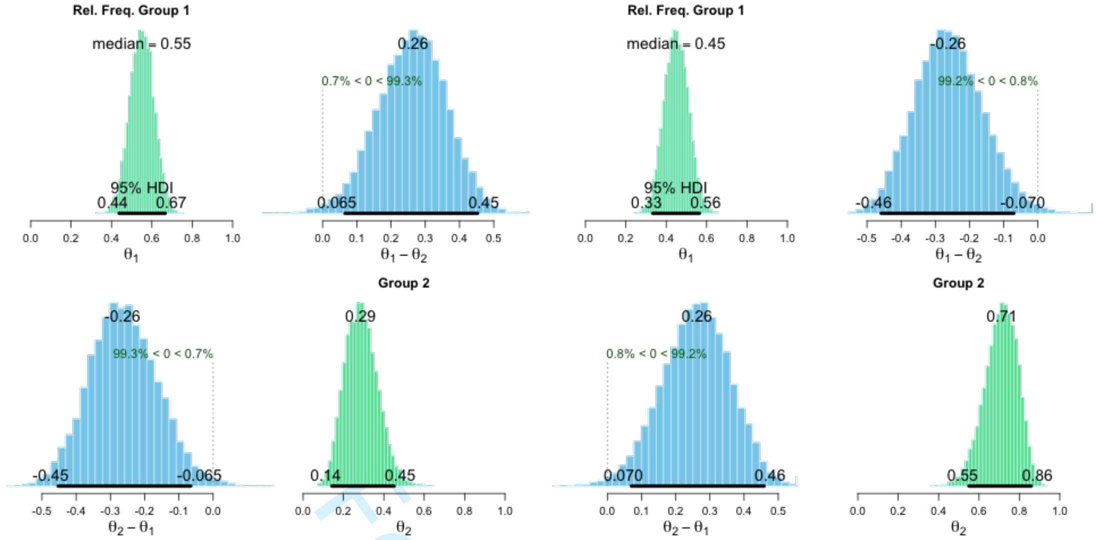

(a) Posterior simulation of knots tied by those with a left hand bias when tested under asocial conditions

(b) Posterior simulation of knots tied by those with a right hand bias when tested under asocial conditions

Figure S7. Posterior simulations of first tying an L or R knot following demonstration given a left-hand bias under asocial conditions. θ_1 refers to those who had a left hand bias under asocial conditions and tied an L knot first following demonstration, θ_2 those who had a left hand bias and tied an R knot first and $\theta_1 - \theta_2$ and $\theta_2 - \theta_1$ the difference between groups. We see there is a larger probability of those who had a left hand bias starting their post-demonstration knot with an L knot than an R. Figure S7b shows the simulations of tying an L or R knot first following demonstration given a right hand bias under asocial conditions. θ_1 refers to those who had a right hand bias under asocial conditions and tied an L knot first following demonstration, θ_2 those who had a right hand bias and tied an R knot first and $\theta_1 - \theta_2$ and $\theta_2 - \theta_1$ the difference between groups. We see there is a larger probability of those who had a right hand bias starting their post-demonstration knot with an R knot than an L.

S5. Recursion Equations

The equations are

$$\begin{aligned} {f'}_{RR} =& f_{RR}((1-g)s^2 + (1-s)^2(1-r)p^2 + (1-s)^2rp + 2(1-g)s(1-s)r) \\ & +2(1-g)s(1-s)(1-r)p \\ & +f_{LL}((1-s)^2(1-r)p^2 + (1-s)^2rp + gs^2 + 2gs(1-s)r) \\ & +2gs(1-s)(1-r)p \\ & +(f_{RL} + f_{LR})((1-s)^2(1-r)p^2 + (1-s)^2rp + s(1-s)r \\ & +s(1-s)(1-r)p) \end{aligned} \tag{S4}$$

$$\begin{aligned} {f'}_{LL} =& f_{RR}(gs^2 + (1-s)^2(1-r)(1-p)^2 + (1-s)^2r(1-p) + 2gs(1-s)r \\ & +2gs(1-s)(1-r)(1-p)) \\ & +f_{LL}((1-g)s^2 + (1-s)^2(1-r)(1-p)^2 + (1-s)^2r(1-p) \\ & +2(1-g)s(1-s)(1-r)(1-p) + 2(1-g)s(1-s)r) \\ & +(f_{RL} + f_{LR})((1-s)^2(1-r)(1-p)^2 + (1-s)^2r(1-p) \\ & +s(1-s)(1-r)(1-p) + s(1-s)r) \end{aligned} \tag{S5}$$

$$\begin{aligned} {f'}_{RL} =& f_{RR}((1-s)^2(1-r)p(1-p) + (1-g)s(1-s)(1-r)(1-p) \\ & +g(1-s)s(1-r)p) \\ & +f_{LL}((1-s)^2(1-r)p(1-p) + (1-g)(1-s)s(1-r)p \\ & +gs(1-s)(1-r)(1-p)) \\ & +f_{RL}((1-g)s^2 + (1-s)^2(1-r)p(1-p) + (1-g)s(1-s)(1-r)) \\ & +f_{LR}(gs^2 + (1-s)^2(1-r)p(1-p) + gs(1-s)(1-r)) \end{aligned} \tag{S6}$$

$$\begin{aligned} {f'}_{LR} =& f_{RR}((1-s)^2(1-r)(1-p)p + (1-g)(1-s)s(1-r)(1-p) \\ & +gs(1-s)(1-r)p) \\ & +f_{LL}((1-s)^2(1-r)(1-p)p + (1-g)s(1-s)(1-r)p \\ & +g(1-s)s(1-r)(1-p)) \\ & +f_{RL}(gs^2 + (1-s)^2(1-r)(1-p)p + gs(1-s)(1-r)) \\ & +f_{LR}((1-g)s^2 + (1-s)^2(1-r)(1-p)p + (1-g)s(1-s)(1-r)) \end{aligned} \tag{S7}$$

S6. EQUILIBRIA EQUATIONS

Equilibria occur when

$$\hat{f}_{RR} = \frac{Q_1}{P}$$

where

(S8)
$$\begin{aligned} Q_1 = {} & -p^2(r-1)(s-1)(1+s(2g-1)(r-1)+rs^2(2g-1))+gs(r(s^2-2)-s) \\ & +p(s-1)(2gs+r^2s(2g-1)(1+s)+r(1+s-2gs(2-s))) \end{aligned}$$

$$\hat{f}_{LL} = \frac{Q_2}{P}$$

where

$$\begin{aligned} Q_2 = {} & s^2(1-g)-p^2(r-1)(s-1)(1+s(2g-1)(r-1)+rs^2(2g-1))-1 \\ & +r(s(1-2g)+s^3(g-1))+p(s-1)(r^2s(2g-1)(1+s) \\ & +2s(g-1)+rs(1+(3-4g)-2s^2(g-1))-2) \end{aligned} \tag{S9}$$

$$\hat{f}_{LR} = \frac{Q_3}{P}$$

where

$$Q_3 = (r-1)(gs-p(s-1)(1+p^2(s-1))(1+(2g-1)(s(r-1)+rs^2))) \tag{S10}$$

$$\hat{f}_{RL} = \frac{Q_4}{P}$$

where

$$Q_4 = (r-1)(gs-p(s-1)(1+p^2(s-1))(1+(2g-1)(s(r-1)+rs^2))) \tag{S11}$$

and

$$P = (1+s)(s(2g-1)(rs-r-1)-1). \tag{S12}$$

S7. Stability

In this system, an equilibrium point is stable if no matter the starting values of f_{RR}, f_{LL}, f_{LR}, f_{RL}, the system comes to rest at the same point. If the point changes depending on these starting values then it is not stable.

To find the stable equilibrium points we set f_{ij} equal to the equilibria points determined by the equations, plus some small perturbation ϵ_{ij}. The equilibrium is stable if the value of f'_{ij}, moves towards the equilibria points given by the equations in Appendix S6.

Let

$$f_{RR} = \frac{Q_1}{P} + \epsilon_{RR} \tag{S13}$$

$$f_{LL} = \frac{Q_2}{P} + \epsilon_{LL} \tag{S14}$$

$$f_{LR} = \frac{Q_3}{P} + \epsilon_{LR} \tag{S15}$$

$$f_{RL} = \frac{Q_4}{P} + \epsilon_{RL} \tag{S16}$$

where Q_i and P are as given in Appendix S6, and

$$\epsilon_{RL} = -\epsilon_{RR} - \epsilon_{LL} - \epsilon_{LR} \tag{S17}$$

to ensure f_{ij} sum to one.

We then compute f'_{RR}, f'_{LL}, f'_{LR}, f'_{RL} and the distance:

$$d_{RR} = f'_{RR} - \frac{Q_1}{P} \tag{S18}$$

$$d_{LL} = f'_{LL} - \frac{Q_2}{P} \tag{S19}$$

$$d_{LR} = f'_{LR} - \frac{Q_3}{P} \tag{S20}$$

$$d_{RL} = f'_{RL} - \frac{Q_4}{P} \tag{S21}$$

We then have the following cases.

Case 1:

$$d_{ij} = 0 \tag{S22}$$

In this case the system jumps to an equilibrium point given by the parameters. The system then remains at this point for all generations. This occurs when $s = 0$. The system is not affected by starting values of f_{ij}, the frequency of each type of knot is determined solely by the values of p and r.

Case 2:

$$d_{ij} = \epsilon_{ij} \tag{S23}$$

In this case there is no change in the system, meaning the system is currently at equilibria, with the system remaining at this point for all generations. This occurs when copying is always accurate and mirroring never occurs, when $s = 1$ and $g = 0$. The equilibrium state is determined by the starting values of f_{ij} and is independent of the values of p and r. The frequency of each type of knot remains constant across generations.

Case 3:

$$d_{ij} < \epsilon_{ij} \tag{S24}$$

In this case the system moves towards the equilibrium point given by the parameters. This occurs when $s < 1$ and the system evolves towards equilibria over generations.

Case 4:

$$d_{ij} > \epsilon_{ij} \tag{S25}$$

In this case the system moves away from the equilibrium point given by the parameters. This never occurs for any equilibrium point in the system, meaning all points are stable.

S8. Barycentric Coordinates

We plot a tetrahedron with vertices at the points $\begin{pmatrix}1\\0\\0\end{pmatrix}$, $\begin{pmatrix}0\\1\\0\end{pmatrix}$, $\begin{pmatrix}0\\0\\1\end{pmatrix}$ and $\begin{pmatrix}1\\1\\1\end{pmatrix}$.

Taking values of f'_{ij} from our equations, we can represent the values of f'_{ij} as points $\mathbf{p}$ inside the tetrahedron using the conversion

$$\mathbf{p} = \begin{pmatrix} f'_{RR} + f'_{RL} \\ f'_{LL} + f'_{RL} \\ f'_{LR} + f'_{RL} \end{pmatrix} \tag{S26}$$

S9. Non-parametric Estimate of Equilibrium State

Following Claidière et al. (2014), we construct a transmission matrix taken directly from the experimental data (Table 1), which represents the probability of the change in knot types from those demonstrated to those learned. For example $x_{2,1} = P(LL|RR)$ is the probability of tying knot LL when shown RR.

$$X = \begin{bmatrix} \frac{14}{26} & \frac{9}{26} & \frac{1}{26} & \frac{2}{26} \\ \frac{9}{25} & \frac{15}{25} & 0 & \frac{1}{25} \\ \frac{4}{24} & \frac{4}{24} & \frac{8}{24} & \frac{8}{24} \\ \frac{6}{25} & \frac{1}{25} & \frac{6}{25} & \frac{12}{25} \end{bmatrix} \tag{S27}$$

X is a right stochastic matrix representing the frequency of change in knots tied given by the experimental data. We can simulate social transmission of these knots within future generations by taking powers of this matrix, basing future generations solely on the present state. This approach treats any parameters affecting change in cultural variant frequency as implicit, linear effects in the transition matrix. After 20 generations we have stability in transmission such that the probability of tying any given knot remains constant (measured to 3 decimal places).

Knot	Parametric	Non-parametric
LL	41.5%	40.1%
RR	41.5%	39.1%
LR	8.5%	7.2%
RL	8.5%	13.6%

Table S6. Percentage of each type of knot at equilibrium predicted by the parametric social transmission model, using ABC-derived mean posterior parameter values, and the non-parametric approach.

Table S6 shows that both the parametric and non-parametric models predict a prevalence of granny over reef knots at equilibrium, but unlike the non-parametric approach, the parametric social transmission model gives equal frequencies of both reef knots. The non-parametric approach makes no theoretical assumptions over how copying fidelity, mirroring, repetition and handedness bias interact so it is unsurprising to find unequal reef knot frequencies. The parametric model behaviour is, by definition, determined by the probabilistic interactions of (s, g, r, p) but the model does not assume that individuals recognise or treat the two reef knots to be mathematically the same. The similarity in the predictions between the parametric and non-parametric approaches indicates that the ABC-derived parameter estimates do a good job at estimating the steady state frequencies derived, using the transition matrix, by the experiment data alone.

S10. Closed System Model

Consider n variants, each of which occurs at frequency f_i, where $\sum_{i=1}^{n} f_i = 1$. Frequencies in the subsequent cultural generation, f', are determined by oblique transmission with copying fidelity s, where failure to copy variant i results in randomly adopting one of the $n-1$ other variants;

$$f_i' = sf_i + (1-s)\frac{(1-f_i)}{n-1}. \tag{S28}$$

The equilibrium frequency $\hat{f}_i = \frac{1}{n}$.

S11. Equilibrium Distribution Given Sampled Parameter Values

The usage of the mean posterior values in Figure 5b results in the grey arrow's smooth evolutionary trajectory. This gives the assumption that the parameter values are constant for each generation, however given the distribution of parameter values seen in Figure 5a it may be more accurate to the sample from that distribution to simulate evolutionary frequencies each generation. Taking parameter values in this way, the result gives evolutionary frequencies distributed around the values resulting from taking the mean posterior values as constant parameter values for each generation, as can be seen in Figure S8.

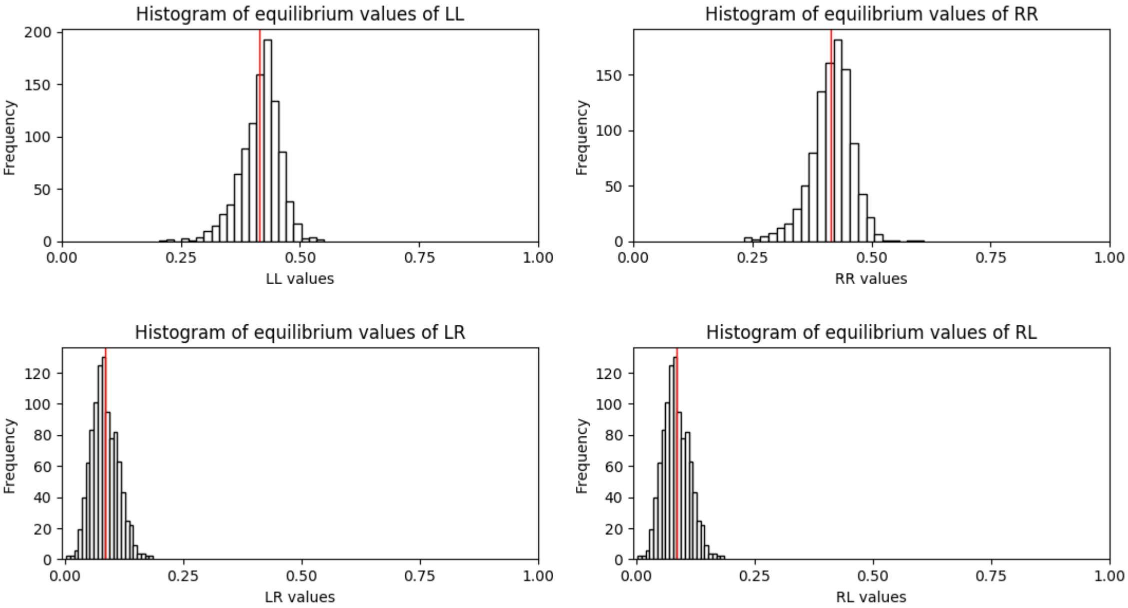

Figure S8. Equilibrium values of LL, RR, LR and RL determined by sampling from the distribution of parameter values. The red lines on each plot denote the equilibrium values determined by taking mean parameter values constant over generations

S12. Knots Frequencies After One Generation Given Sampled Parameter Values

The equilibrium frequencies in Figure 5b demonstrate the prevalence of granny knots over reef knots in the population when simulated over generations, but sampling from the posterior distribution for the parameters p, g, r and s allows us to explore the relative occurrence of each knot in one generation. Sampling from the posterior of parameter values in a way that models the experiment gives the frequency of each type of knot. In Figures S9a and S9b we show the frequency of each knot type over repeated simulations with the maximum occurrence for each knot being 25 to represent the demonstrations in the experiment. We see that both granny knots, RR and LL, occur much more frequently than the reef knots LR and RL.

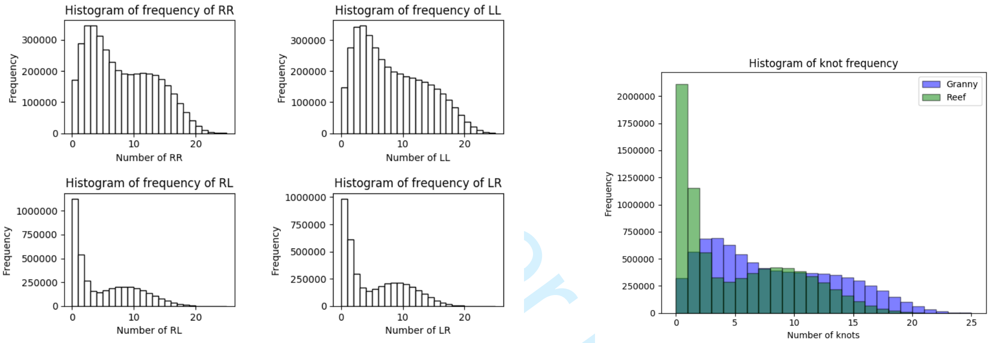

(a) (b)

Figure S9. Part (a) shows the frequencies of LL, RR, LR and RL after one generation determined by sampling parameter values from the posterior distribution. We see that this results in higher occurrences of the knots RR and LL than RL and LR. Part (b) shows the frequencies of granny and reef knots after one generation determined by sampling parameter values from the posterior distribution. We see that this results in higher occurrences of the knots granny knots over the reef with the frequency of each type of knot overlayed.

References

Rasmus Bååth. Bayesian First Aid: A Package that Implements Bayesian Alternatives to the Classical * .test Functions in R. In *UseR! 2014 - Int. R User Conf.* 2014.

Robert C Chisnall. Knot-tying habits, tier handedness, and experience. *J. Forensic Sci.*, 55(5):1232–1244, 2010. ISSN 00221198. doi: 10.1111/j.1556-4029.2010.01451.x.

Nicolas Claidière, Thomas C Scott-Phillips, and Dan Sperber. How Darwinian is cultural evolution? *Philos. Trans. R. Soc. B Biol. Sci.*, (March), 2014.

Andrew Gelman, John B Carlin, Hal S Stern, and Donald B Rubin. *Bayesian Data Analysis*, volume 2. Chapman and Hall/CRC, 3 edition, 2003. ISBN 158488388X. doi: 10.1017/CBO9781107415324.004.

Vaughan F R Jones. A polynomial invariant for knots via Von Neumann algebras. *Bull. Am. Math. Soc.*, 12(1):103–111, 1985. ISSN 02730979. doi: 10.1090/S0273-0979-1985-15304-2.